Available online at www.sciencedirect.com
ScienceDirect
Ceramics International 34 (2008) 1893–1902
CERAMICS INTERNATIONAL
www.elsevier.com/locate/ceramint

An alumina–YAG nanostructured fiber prepared from an aqueous sol–gel precursor: Preparation, rheological behavior and spinnability

M. Shojaie-Bahaabad [a], E. Taheri-Nassaj [a,*], R. Naghizadeh [b]

[a] Department of Materials Science and Engineering, Tarbiat Modares University, P.O. Box 14115-143, Tehran, Iran
[b] Department of Materials Science and Engineering, Iran University of Science and Technology, P.O. Box 16846-13114, Tehran, Iran

Received 22 January 2007; received in revised form 14 May 2007; accepted 2 July 2007
Available online 22 August 2007

Abstract

Continuous-fiber development is needed for high-performance and high-temperature composites. Various methods have been used to make ceramic fibers. In this research, composite fibers (YAG/Al_2O_3) were synthesized from an aqueous solution of aluminum powder, aluminum chloride hexahydrate and yttrium oxide by the sol–gel method. Transparent fibrous gels were obtained by immersing a thin wire into the viscous sol, then pulling it out by hand. Rheological measurements suggested that the sols exhibited spinning when they were viscous and Newtonian or near Newtonian to the time of gelation. The sols became non-spinnable when thixotropic flow behavior was observed. It was observed that the time of hydrolysis–condensation, drawing, gelation and length of the gel fibers decreased with increasing the amounts of either acid or yttrium oxide. The time of hydrolysis–condensation and gelation decreased with increase in the amount of aluminum powder, whereas the time of drawing and spinnability increased. The desired viscosity of the sols for spinning was between 2000 and 5000 P. The dried gel fibers had a smooth surface with diameter ranging from 20 to 200 μm. The composite fiber showed fine-grained microstructure (100–200 nm) after heat treatment at 1400 °C.

Keywords: A. Sol–gel processing; Al_2O_3/Y_2O_3 composite gel fibers; Rheological properties; Spinnability

1. Introduction

The demand for materials with high-mechanical and thermal performance has been led to the development of metal and ceramic matrix composites (MMC_s and CMC_s). In fiber reinforced CMC_s, ceramic fibers are interested as reinforcement because of their favorable mechanical, physical and chemical properties [1–3]. Methods such as melt spinning [4–6], Taylor processing [7,8], relic processing [9,10], unidirectional freezing [11], slurry spinning [10,11], viscous sol spinning [7,10], CVD [5] and sol–gel processing [5,11–13] have been employed to obtain ceramic fibers.

Among the inorganic fibers, ceramic oxide fibers are suitable candidates due to their high thermo-mechanical stability and resistance to both oxidizing and reducing atmosphere at high temperatures [14]. Commercially available oxide fibers are alumina fibers. However, applications of these fibers are limited because of the degradation in their strength and creep properties above 1000 °C [15].

It has been reported that the creep resistance of polycrystalline ceramics can be improved by the addition of hard second phase particles [16]. Yttrium–aluminum garnet (YAG, $Y_3Al_5O_{12}$) is a prime candidate for the hardening of alumina due to its excellent creep resistance and its high-melting point (1940 °C) [15]. In the composite fibers of alumina/mullite which have a microstructure of fine alumina grains dispersed in a matrix of mullite grains, an enhanced creep resistance has been observed comparing to the mullite fibers [17,18]. It is therefore expected that YAG/alumina fibers might exhibit more high strength and creep resistance than alumina and YAG fibers.

YAG/Al_2O_3 composite fibers have been fabricated by methods such as edge-defined film-fed growth (EFG), laser-heated float zone (LHFZ) [19], solidified eutectic melts [4] and sol–gel process.

In the sol–gel process, fibers can be prepared from alkoxide precursors and chloride or nitrate salts. Using alkoxide precursors is very popular for producing fibers, but it requires several steps to obtain spinnable sols. Thus, this method

* Corresponding author.
E-mail address: taheri@modares.ac.ir (E. Taheri-Nassaj).

0272-8842/$34.00
doi:10.1016/j.ceramint.2007.07.032

requires long time and much money to synthesize fibers. This problem is minimized for salt precursors.

The aim of the present work is preparing of composite gel fibers by a sol–gel method using aluminum chloride salt, aluminum and yttrium oxide powders in aqueous system. The rheological behavior and spinnability of the sols were also investigated. Further, the effect of aluminum and yttrium oxide content and acidification of the precursor sols on the drawing and macroscopic properties of the sols were analyzed. In this research, no organic additives were used to stabilize the sols or to improve their spinnability. This is because of preventing their possible side effects on the properties of products.

2. Experimental procedure

2.1. Starting materials

The starting materials used for preparing the precursor sols were aluminum chloride hexahydrate ($AlCl_3{\cdot}6H_2O$), aluminum powder, yttrium oxide (Y_2O_3) and hydrochloric acid. The aluminum chloride hexahydrate was obtained from Merck Co. (number 101084 and purity >97%). Some properties of this salt are mentioned in Table 1. The aluminum powder was produced by M.A. University. This powder has a spherical shape (Fig. 1) with an average diameter about 37.5 μm (Fig. 2). Its impurity ($Fe_2O_3 + SiO_2 + \cdots$) is less than 0.5 wt.% (Table 2). The yttrium oxide with a molar mass of 225.81 g/mol and a density of 5.01 g/cm^3 was provided by Sigma–Aldrich Co. Its purity was 99.99%. Hydrochloric acid (1 mol/l) was obtained from the domestic producers in Iran.

2.2. Preparation of the precursor sol

In the present study, composite gel fibers (Al_2O_3/Y_2O_3) were prepared through sol–gel spinning. At first, the calculated amount of yttrium oxide was dissolved in aqueous HCl and mixed with distilled water. Then the required amounts of aluminum chloride hexahydrate and aluminum powder were added to the sol. Addition of aluminum powder to the sol was carried out with 0.78 g/min rate. The precursor sol was heated and stirred with 400 1/min rate at 98 °C for 2–6 h to completely dissolve the starting materials. The molar ratio of aluminum powder to aluminum salt was varied from 0.53 to 9.14 and the molar ratio of acid to water was selected between 0 and 0.36. The yttrium oxide weight percent (0, 2, 4, 6, 8, and 10 wt.%) was also varied to study the macroscopic properties of the precursor sols.

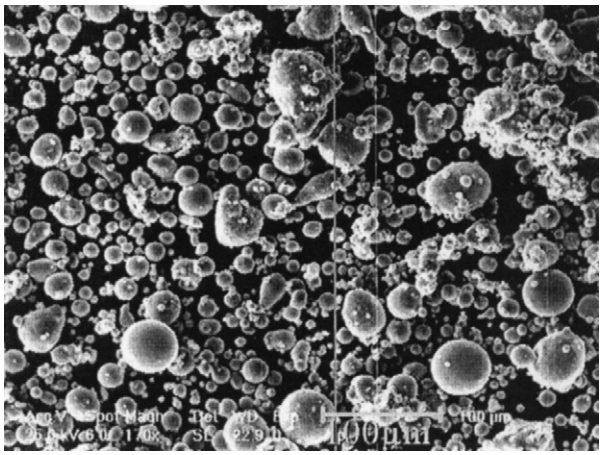

Fig. 1. SEM micrograph of aluminum powder.

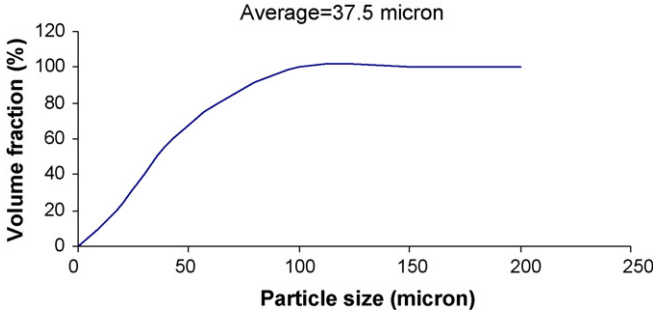

Fig. 2. Particle size distribution of aluminum powder.

2.3. Preparation of the gel fibers

After stirring, the precursor sol was kept open and concentrated by evaporating the solvent at ambient temperature (~25 °C). When the sol reached to appropriate viscosity for spinning, the gel fibers were prepared by immersing a thin stainless steel wire into the condensed precursor sol and pulling it out slowly by hand. The fibers drawing speed was set to about 3–4 cm/s and the fibers could be drawn in condition of about 50% relative humidity at room temperature.

2.4. Preparation of the composite ceramic fibers

The gel fibers were dried at 45 °C for 24 h in an oven. They were then put in an alumina plate and heat treated in air at different temperatures. Heat treatment was carried out at

Table 1
Properties of aluminum chloride hexahydrate as Merck product

Thermal decomposition temperature	100 °C
Melting point	~100 °C
Solubility in water at 20 °C	1330 g/l
pH	~2.5 (50 g/l, water, 20 °C)
Color	Colorless
Form	Solid
Molar mass	241.43 g/mol
Density at 20 °C	2.4 g/cm^3

Table 2
Chemical analysis of aluminum powder

Element	wt.%
Al	99.63
Fe	0.23
Si	0.12
Ca	0.01
Zn	0.01

Table 3
Effect of the concentration of aluminum powder on the macroscopic properties of the precursor sols

Sols	$Al/AlCl_3$ (molar ratio)	HCl/H_2O (molar ratio)	Y_2O_3 (wt.%)	Initial PH of precursor sol	Appearance of sol	Hydrolysis–condensation time (h)	Fiber drawing time (h)	Gelation time (h)	Spinnability
A1	9.14	0.18	6	4.35	Gray-opaque	–	–	0.5	Xerogel-opaque
A2	7.02	0.18	6	4.25	Gray-opaque	–	–	1.5	Xerogel-opaque
A3	5.43	0.18	6	4	Gray-opaque	–	–	3	Xerogel-opaque
A4	3.54	0.18	6	3.8	Gray-translucent	–	–	4.5	Xerogel-opaque
A5	1.81	0.18	6	3.2	Silver gray-transparent	7.5	2.5	12	70–80 cm, transparent thin, soft, glass like
A6	1.45	0.18	6	3.1	Silver gray-transparent	8.25	1.45	16.5	20–30 cm, transparent thin, soft, glass like
A7	1.06	0.18	6	3	Transparent	8.92	1.2	20	15–20 cm, transparent thin, soft, glass like
A8	0.87	0.18	6	2.8	Transparent	9.35	0.78	23.5	10 cm, transparent, very thin, soft, glass like
A9	0.53	0.18	6	2.5	Transparent	–	–	26	Xerogel-yellow

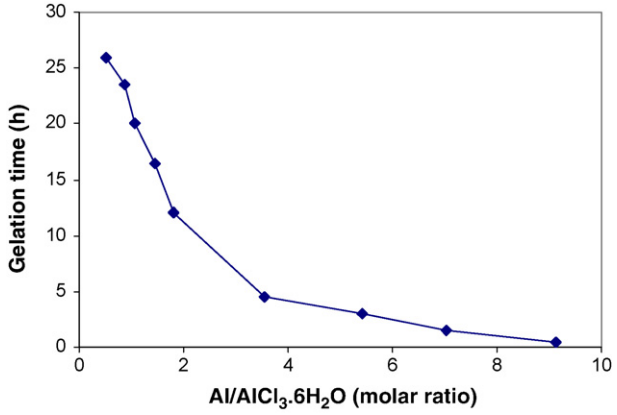

Fig. 3. Gelation time of the sols with different aluminum powder contents.

temperature ranging from 500 to 1500 °C with a heating rate of 10 °C/min. The holding time at the desired temperature was fixed at 4 h. The fibers were then cooled in the furnace.

2.5. Characterization

After stirring and heating, pH of the precursor sols was measured using pH-meter (Jenwey, Model 3520) at room temperature. In order to estimate the progress of hydrolysis and condensation reactions of the precursor sols, the interval time between the acid addition into the precursors and the moment at which the sols reached to the appropriate viscosity for pulling of fibers was determined [20,21]. Spinnability of the sols was estimated from the length of the gel fibers drawn from the spinnable condensed sols. Fiber drawing time of the spinnable precursor sols was obtained by measuring the interval time between the beginning and the end of the complete pulling of the fibers [20,21]. Gelation of the precursor sols was estimated by a qualified method. In this method, gelation time was determined by turning the reaction vessel upside down until no sol can flow out of the vessel at room temperature [22]. Since there might be a relation between the gelation time and the volume of the sol and the size of the vessel, all the experiments of the present study were implemented in the same glass vessel and with the same total volume. The viscosity of the precursor sols was measured using a Brookfield viscometer (Model DV-II+) at room temperature. X-ray diffraction test (XRD) was performed with the X-ray diffraction spectroscopy (Philips; XPERT model) to identify the crystal structure of fibers at different heat treatment temperatures. Microstructure features were observed under a scanning electron microscope (Philips; XL30 model).

Table 4
Effect of the concentration of acid on the macroscopic properties of the precursor sols

Sols	$Al/AlCl_3$ (molar ratio)	HCl/H_2O (molar ratio)	Y_2O_3 (wt.%)	Initial PH of precursor sol	Appearance of sol	Hydrolysis–condensation time (h)	Fiber drawing time (h)	Gelation time (h)	Spinnability
B1	1.81	0	6	4.5	Opaque	–	–	23	Xerogel-opaque
B2	1.81	0.08	6	4.1	Gray-opaque	–	–	18.5	Xerogel-opaque
B3	1.81	0.12	6	3.8	Gray-opaque	–	–	14.4	Xerogel-opaque
B4	1.81	0.22	6	2.8	Gray-transparent	5	1	9.5	30–40 cm, transparent thin, soft, glass like
B5	1.81	0.26	6	2.2	Gray-translucent	1.45	0.4	6.7	10–20 cm, transparent thin, soft, glass like
B6	1.81	0.32	6	1.8	Opaque	–	–	3.2	Xerogel-opaque
B7	1.81	0.36	6	1.5	Opaque	–	–	1.75	Xerogel-opaque

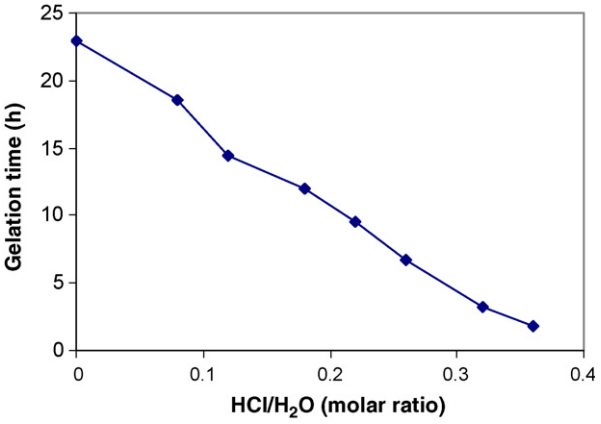

Fig. 4. Gelation time of the sols with different acid contents.

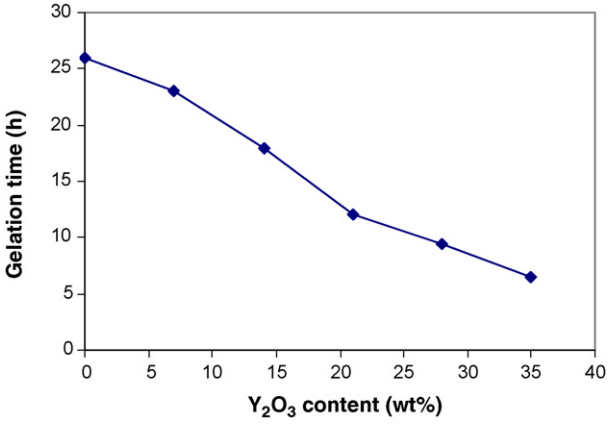

Fig. 5. Gelation time of the sols with different Y_2O_3 contents.

3. Results and discussion

Yttrium oxide was firstly dissolved in acid and formed yttrium chloride. Then, the obtained salt was hydrolyzed with water and formed yttrium hydroxide. The chemical reactions can occur as follows:

$$Y_2O_3 + 6HCl \rightleftarrows 2YCl_3 + 3H_2O \quad (1)$$

$$2YCl_3 + 6H_2O \rightleftarrows 2Y(OH)_3 + 6HCl \quad (2)$$

Hydrolysis reactions occurred because water molecules coordinated to metal ions were more acidic than in the non-coordinated state due to charge transfer from the oxygen to the metal atom [23]. Aluminum chloride hexahydrate was also hydrolyzed with water and formed aluminum hydroxide in hydrochloric acid sol. To increase the Al^{3+} content of the sol, aluminum powder was dissolved during the stirring and heating. The chemical reaction equations are [24]

$$AlCl_3 + 3H_2O \rightleftarrows Al(OH)_3 + 3HCl \quad (3)$$

$$Al + 3HCl \rightleftarrows AlCl_3 + 1.5H_2 \quad (4)$$

Therefore, yttrium and aluminum hydroxides were formed in the precursor sols after hydrolysis reactions.

3.1. Characterization of the macroscopic properties of the precursor sols

3.1.1. The effect of aluminum powder

Microscopic properties of the sols prepared with different amounts of aluminum powder are shown in Table 3. Since aluminum powder is cheaper than aluminum chloride, economically it is better to increase $Al/AlCl_3$ ratio so that we can make the stable sol. According to reaction (4), aluminum consumed HCl produced from hydrolysis of the aluminum salt. Hence, production of aluminum chloride by dissolving the aluminum metal promoted the hydrolysis and condensation reactions and inhibited the promotion of reaction (3) to the left.

As shown in Table 3, the sols consisting of high aluminum powder content (with a molar ratio $Al/AlCl_3{\cdot}6H_2O$ higher than 1.81) were opaque because the acid content was not enough to dissolve aluminum metal powder completely. In this range, solubility of the aluminum powder was very limited and sols were non-spinnable. As the aluminum content was decreased, transparency of the sols increased (Table 3) and the water required for dissolving of the aluminum powder decreased. When the molar ratio of aluminum metal to aluminum salt was low (<0.87), hydrolysis and condensation reactions were not completely occurred and the sols were non-spinnable.

Table 5
Effect of the concentration of yttrium oxide on the macroscopic properties of the precursor sols

Sols	$Al/AlCl_3$ (molar ratio)	HCl/H_2O (molar ratio)	Y_2O_3 (wt.%)	Initial PH of precursor sol	Appearance of sol	Hydrolysis–condensation time (h)	Fiber drawing time (h)	Gelation time (h)	Spinnability
C1	1.81	0.18	0	4.3	Silver gray-transparent	18.5	3	26	80–100 cm, transparent, thick, hard, glass like
C2	1.81	0.18	2	4.1	Silver gray-transparent	–	–	23	Xerogel-opaque
C3	1.81	0.18	4	3.8	Silver gray-transparent	–	–	18	Xerogel-opaque
C4	1.81	0.18	8	2.7	Gray-opaque	4.6	1.4	9.5	70–80 cm, transparent thick, hard, glass like
C5	1.81	0.18	10	2.5	White-opaque	2.7	1	6.5	20–30 cm, transparent thick, hard, glass like

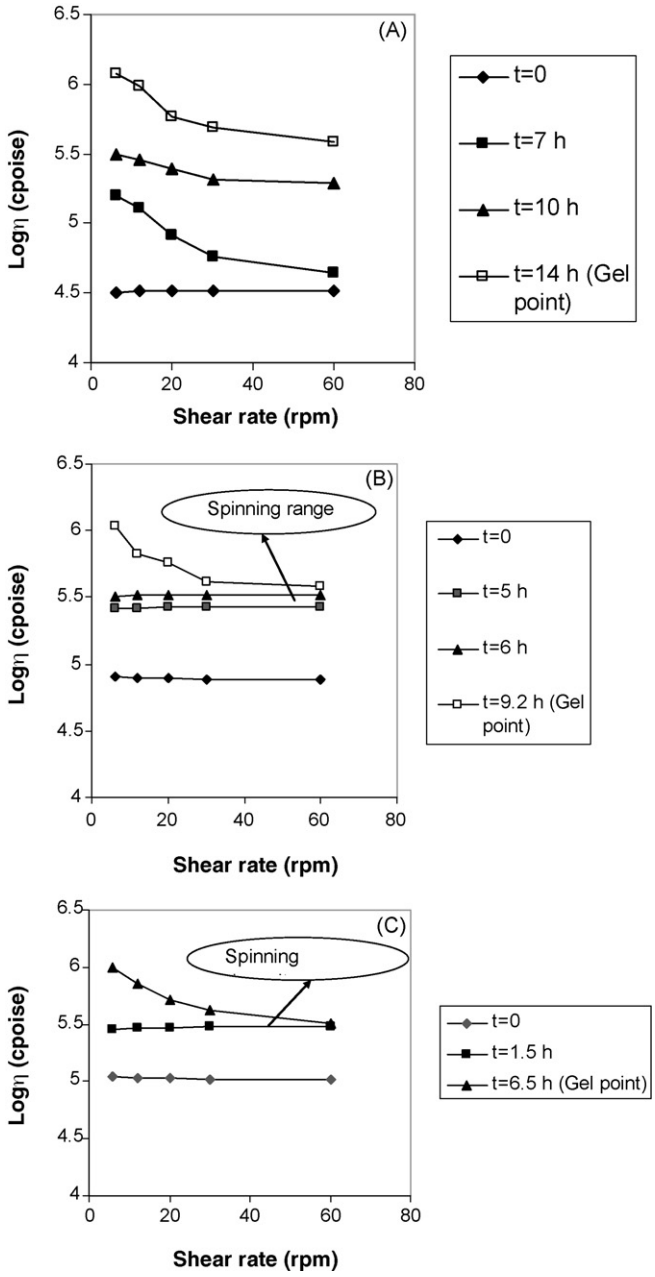

Fig. 6. Dependence of viscosity on shear rate for the sols prepared with different amounts of acid obtained from various reaction times at 25 °C: (A) sol B3; (B) sol B5 and (C) sol B6.

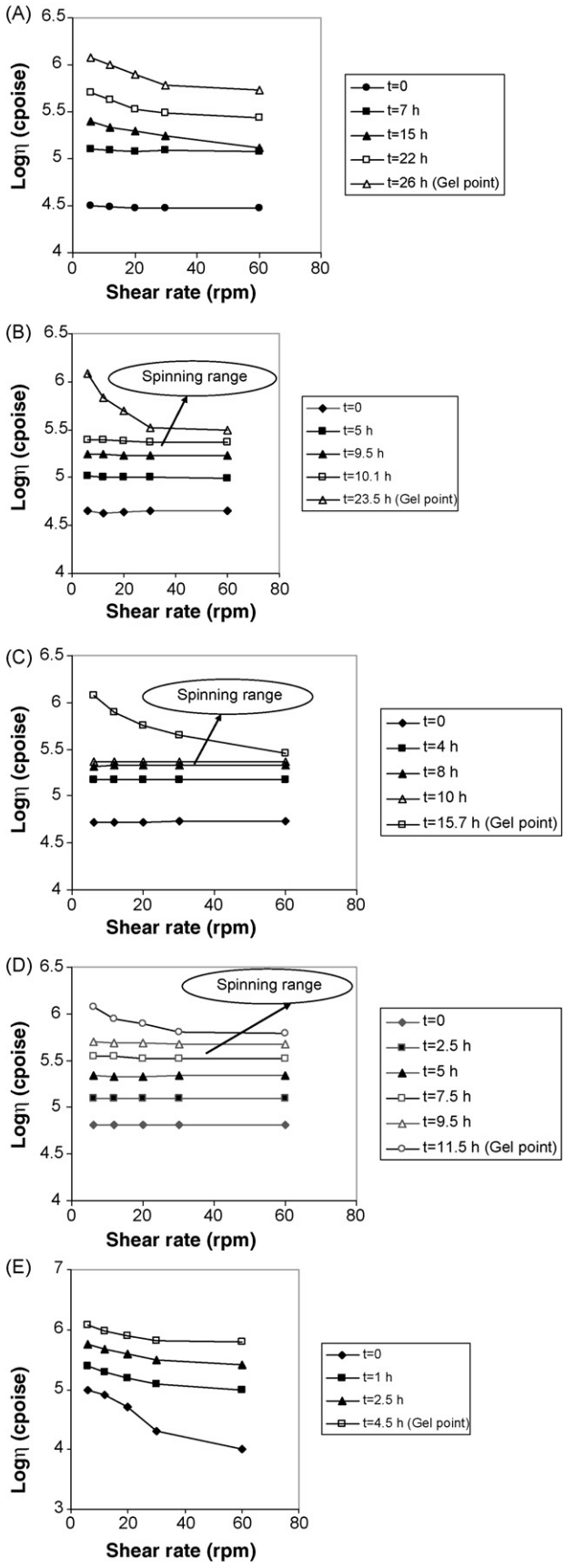

Fig. 7. Dependence of viscosity on shear rate for the sols prepared with different amounts of Al powder obtained from various reaction times at 25 °C: (A) sol A9; (B) sol A8; (C) sol A6; (D) sol A5 and (E) sol A4.

The gel fibers could be obtained from the viscous sols in the composition range of $Al/AlCl_3{\cdot}6H_2O$ molar ratio of 0.87–1.81 (Table 3). In this range, pH varied from 2.8 to 3.2 and solubility of the aluminum powder for drawing fibers was enough. According to Fig. 3 and Table 3 by increasing aluminum content, hydrolysis–condensation and gelation time decreased, whereas fiber drawing time and spinnability increased.

When metal salts are dissolved in water, the cationic metal complex $[M(H_2O)_6]^{3+}$ exists only below pH 3. As the pH is increased, the water ligands are deprotonated and the ions

$[M(OH)_N(H_2O)_{6-N}]^{(3+Z)+}$ are formed, where M is defined as metal, N as a coordination number and Z as charge. Mononuclear species are only stable in very dilute sols. At higher concentrations, polynuclear species are formed by condensation reactions (olation and oxolation) and formation of M–OH–M and M–O–M with linear or non-linear links [23]. The chain like or linear type species were well known to be required for drawing fibers, while the formation of three-dimensional network structures would be favorable for the bulk or monolithic gels [25].

The viscous sols (A5–A8) showed the spinnability. It can be suggested that some kinds of linear species might have been formed in the spinnable sols and were then grown linearly to near the gelation time. Namely, the longer gel fibers could imply to higher degree of the spinnability of the precursor sols. It reflects the formation of the species with more chain like or linear type structures and/or with less branched or cross-linked structures in the spinnable sols. As a result, longer linear chains were probably formed with further dissolving aluminum powder in the sols. Therefore, the obtained gel fibers in the spinning range could be longer.

Spinnability of the sols was remarkably dependent on the dissolved content of the aluminum powder. The addition of an appropriate amount of aluminum powder to the precursor sols promoted the formation of linear structures and improved the spinnability. By dissolving more aluminum powder, the hydrolysis–condensation reactions could be promoted and the amounts of the linear chains increased in the sols. Therefore, entanglement of the chains and possibility of the formation of three-dimensional structures rather than linear structures could be caused to decrease spinnability, hydrolysis–condensation and gelation times. By further addition of aluminum powder, it cannot be dissolved and precipitated in the sol.

3.1.2. The effect of acid

Characteristics of the precursor sols prepared with different amounts of acid are summarized in Table 4. It was observed that appearance of the sols was dependent on the acid content. When the molar ratio of acid to water was less than 0.18, the sols were gray-opaque. This is because the solubility of aluminum and yttrium oxide powders was limited. It therefore resulted in an insufficient hydrolysis. By increasing the amount

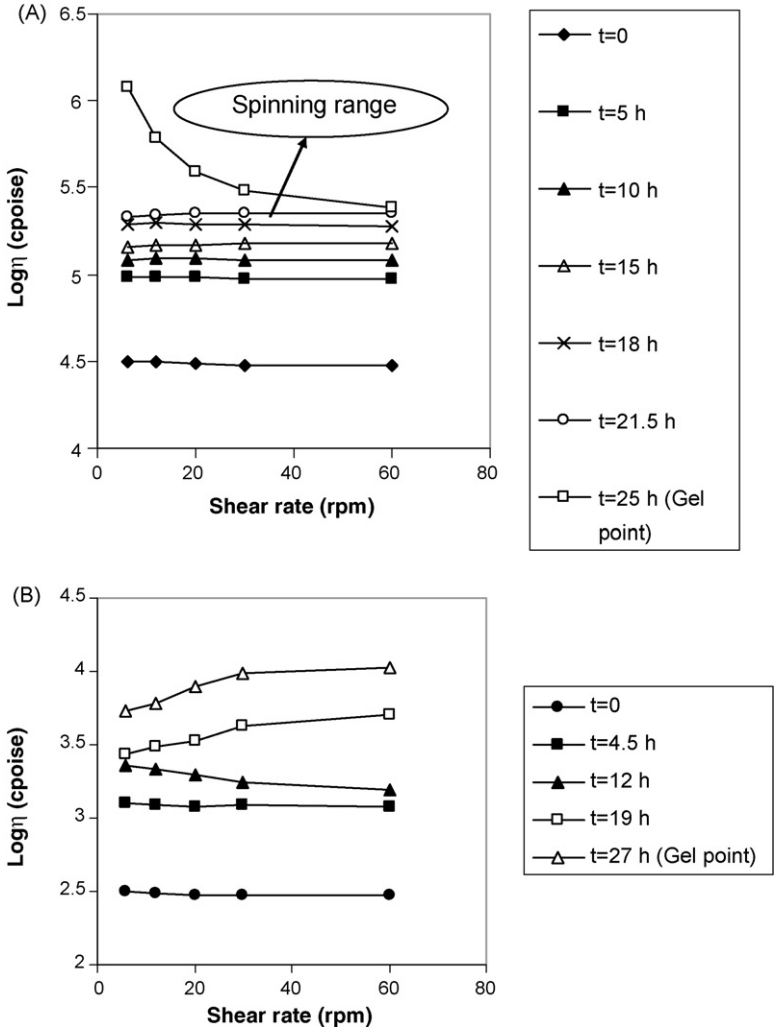

Fig. 8. Dependence of viscosity on shear rate for the sols prepared with different amounts of yttrium oxide obtained from various reaction times at 25 °C: (A) sol C1; (B) sol C2; (C) sol C3; (D) sol C4 and (E) sol C5.

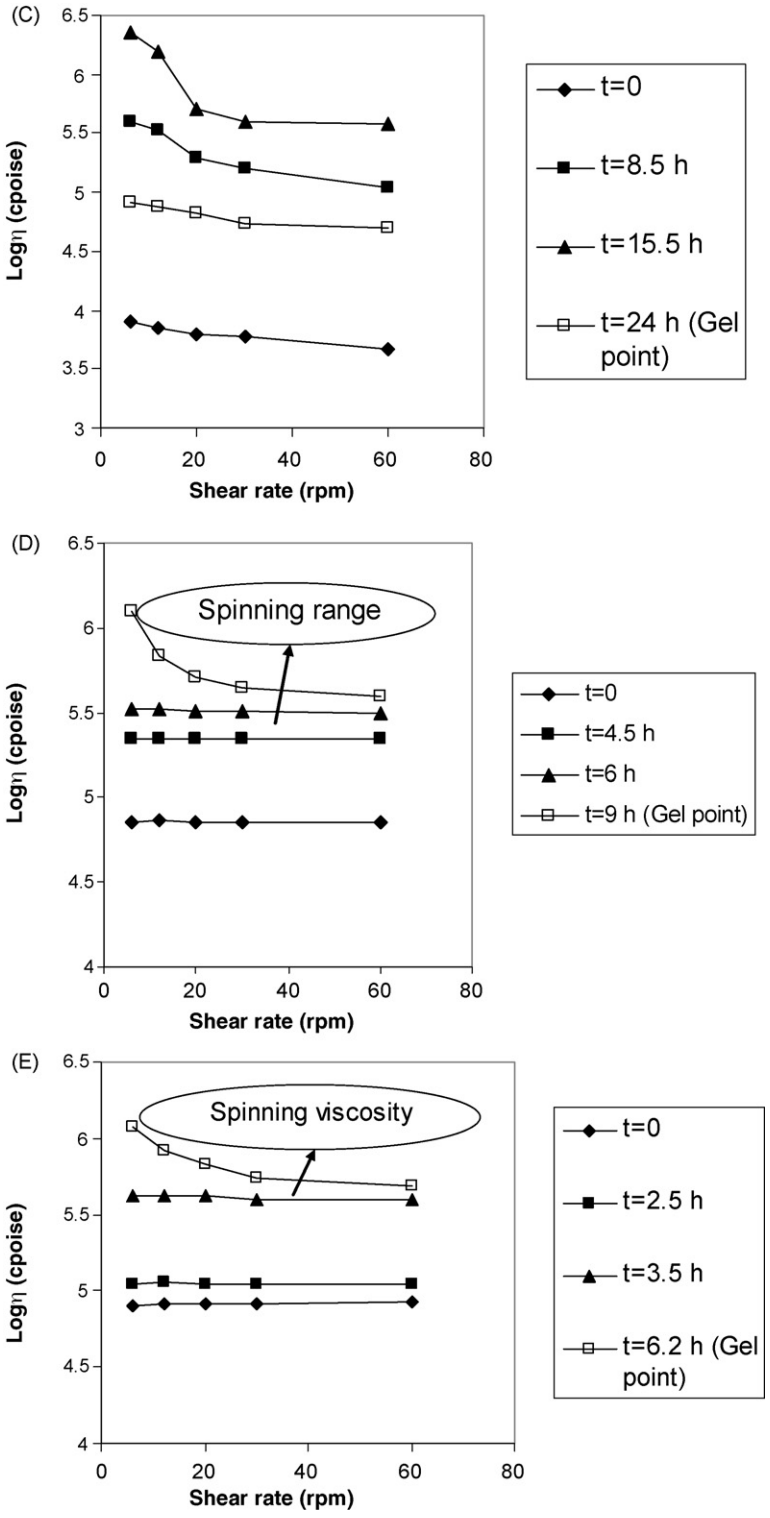

Fig. 8. (*Continued*).

of acid to water up to molar ratio, transparency of the sols increased. This is due to increasing the solubility of components. However, with increasing the amount of acid to water up to 0.36 mol ratio, transparency of the sols again decreased and appearance of the sols was opaque (Table 4). This is because the hydrolysis–condensation rate and heterogeneity of the sols increased.

In most systems, hydrolysis–condensation reactions rapidly proceed when acid catalyst (HCl) is employed [25,26]. Therefore, according to Fig. 4, the gelation time decreased with the acid content.

It was impossible to draw out the fibers from the precursor sols without acid. The use of acid increased the solubility of the components in the precursor sols and resulted in reactions

between the dissolved ions which led to linear chains. Depending on the amount of acid, the pH of the sols varied between 4.5 and 1.5. The spinnability and fiber drawing time were strongly dependent on the concentration of the acid in the range of spinning (pH ranging from 2.2 to 3.2). As the pH of the sols increased, length of the drawn fibers increased. The longest fibers were obtained for pH 3.2 (Table 4).

Type of the species formed in the sols could be estimated through measuring the spinnability and length of the drawn gel fibers. Thus, the longer fibers showed that longer linear chains were formed in spinnable sols. The higher acid content significantly promoted the hydrolysis–condensation reactions and thus enhanced the degree of branching of the chains by chain–chain reactions. It therefore resulted in decreasing the length of gel fibers and the fiber drawing time in the range of spinning.

3.1.3. The effect of yttrium oxide

Table 5 shows the effect of yttrium oxide content on macroscopic properties of the sols. pH of the obtained sols consisting of different amounts of yttrium oxide varied between 4.3 and 2.5. As shown in Table 5, transparency of the sols decreased with yttrium oxide content. The solubility of the components decreased with increasing yttrium oxide content, because the amount of acid was constant.

Furthermore, fiber drawing, gelation and hydrolysis–condensation times and the fiber length decreased with yttrium oxide content (Table 5 and Fig. 5). It seems that increasing the amount of yttrium oxide might caused more rapid hydrolysis–condensation and formation of three-dimensional framework structures in the sols.

For continuous production, we need a condition in which adequate fiber drawing time (t_f) is obtained along with minimized gel time (t_g). The ratio of t_f to t_g gives an indication of this condition or usefulness of the sols [22]. According to this notice, the sol A5 was selected as favorite composition for the practical production.

3.2. Characterization of rheological properties of the precursor sols

Spinnability of the precursor sols was related to their rheology and viscosity. According to literatures, the sols must have Newtonian behavior. When linear polymerization takes place in the sols and viscosity becomes independent on rotating speed, the sols can be spinnable. While three-dimensional

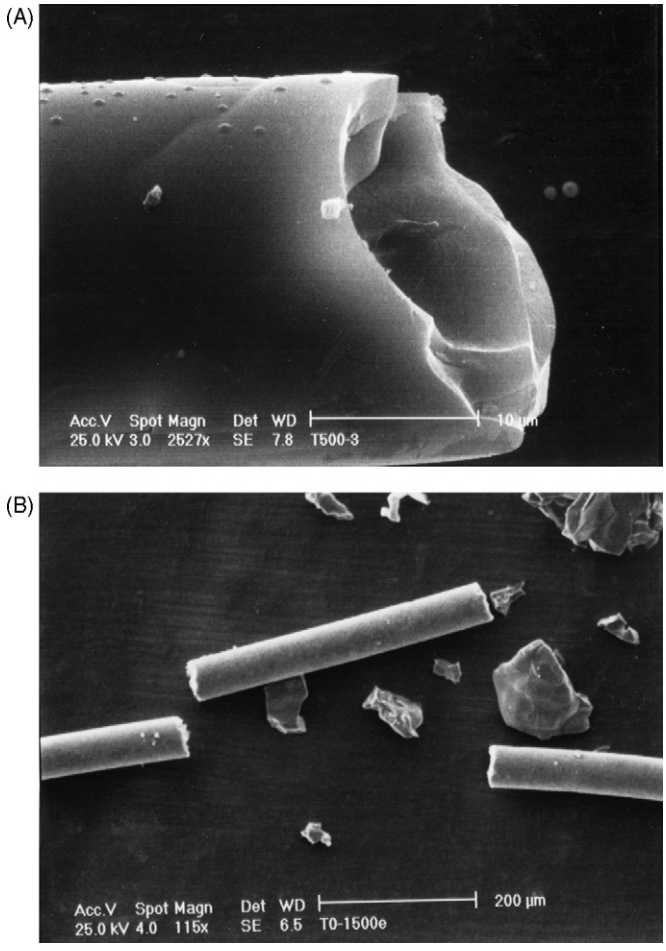

Fig. 9. SEM micrograph of the gel fibers obtained from the sols: A (A5) and (B) C1 after drying.

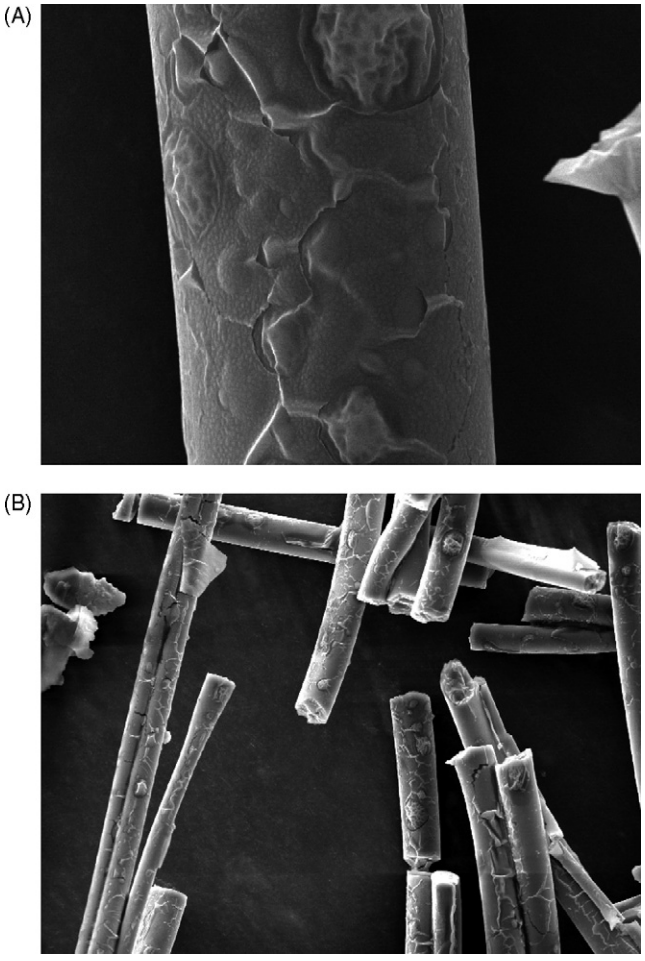

Fig. 10. SEM micrograph of the gel fibers obtained from the sols: A (A5) and B (C5) after aging at ambient temperature.

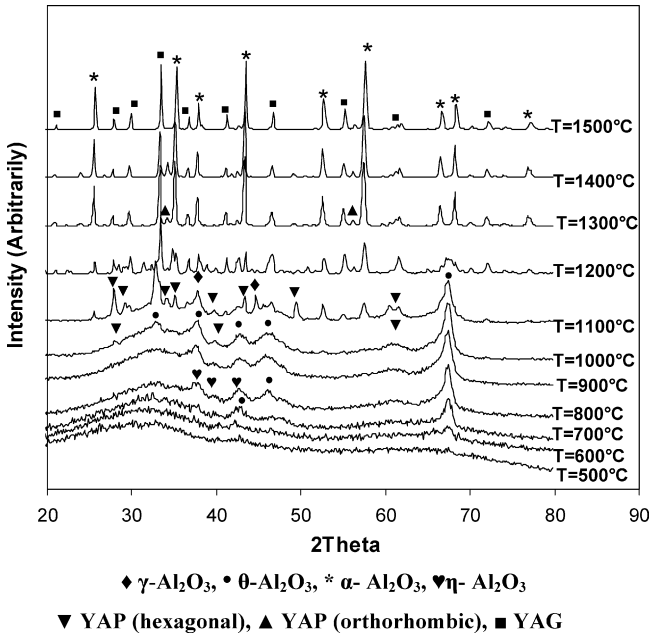

Fig. 11. XRD pattern of the composite fibers obtained from the sol A5 heat treated at different temperatures for 4 h.

polymerization takes place in the sols the fiber cannot be produced [27–31].

Rheological behaviors of the sols consisting of different amounts of acid, aluminum and yttrium oxide powders are shown in Figs. 6–8. All of the sol samples were kept open to ambient atmosphere in the present study, thus increased viscosity could be attributed to the evaporation and hydrolysis–condensation reactions of the sols.

The increase of acid, yttrium oxide and aluminum powders caused to increase the initial sols viscosity. It also results in increased viscosity of the sols more rapidly up to gelation. This is because the formation of network structures in the sols was promoted due to increased rate of hydrolysis–condensation. As shown in Figs. 6–8, the spinnable sols behaved as Newtonian fluid in the initial steps of hydrolysis–condensation reactions. These sols exhibited Newtonian behavior up to high viscosities ranging from 2000 to 5000 P, where fibers could be drawn. They then exhibited non-Newtonian (thixotropic) behavior up to complete gelation.

Two behaviors were observed in the non-spinnable sols. Some sols behaved as thixotropic fluid from beginning. Other sols behaved as Newtonian fluid at first and then behaved as non-Newtonian fluid at high viscosities. These sols did not have enough viscosity to be spinnable.

The gelation process of the sols involves both simultaneous reactions of hydrolysis and condensation. Due to these reactions, a linear chain structure was first formed in the spinnable sol. This structure was then transformed to three-dimensional network during gelation. The increase of viscosity in the Newtonian behavior range can be attributed to an increase in the concentration of the linear throughout the sols. On the other hand, the increased viscosity in the non-Newtonian behavior range can be related to formation of three-dimensional network structures in the sols.

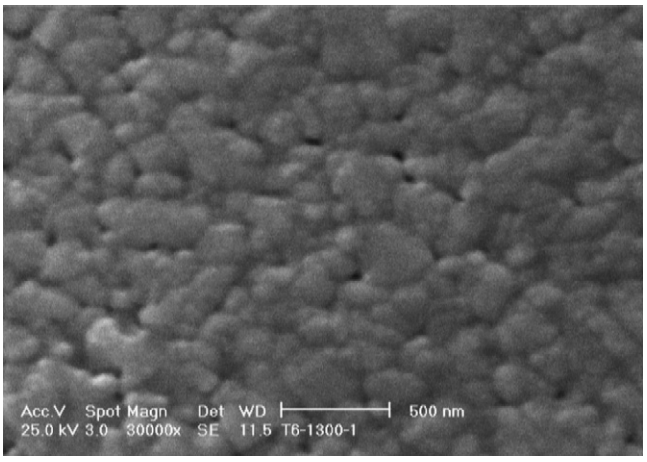

Fig. 12. SEM micrograph of the composite ceramic fiber (YAG: 21 wt.%) obtained from the sol A5 heat treated at 1400 °C for 4 h.

Fig. 9 shows SEM micrographs of the gel fibers. As shown, the gel fibers had smooth and dense appearance without large pores with diameter ranging from 20 to 200 μm after drying at room temperature. All of the drawn gel fibers were flexible and tough after drawing. They became brittle and fragile after aging at room temperature. Their surfaces were uniform after aging indicating that further polycondensation might be occurred (Fig. 10).

3.3. Phase transformation and microstructure of the composite ceramic fibers

Fig. 11 shows XRD patterns of obtained gel fibers from the optimum sol (A5) at different temperatures. As can be seen, the gel fibers (6 wt.% yttrium oxide) heat treated at 500 °C for 4 h were amorphous. The first crystalline phase, θ-Al_2O_3, was formed with increasing the temperature of heat treatment up to 700 °C. Some peaks related to γ-Al_2O_3 and η-Al_2O_3 phases were detected in the gel fibers heat treated at 900 °C. Hexagonal YAP (Y_2O_3·Al_2O_3) was crystallized above 1000 °C. Furthermore, crystallization of the α-Al_2O_3 and YAG phases were started at 1100 °C. Hexagonal YAP was transformed to orthorhombic YAP with increasing temperature. The relative intensity of YAG and α-Al_2O_3 peaks increased up to 1400 °C and YAP completely disappeared simultaneously.

As shown in Fig. 12, the fibers had a fine-grained microstructure ranging from 100 to 200 nm after heat treatment at 1400 °C.

4. Conclusion

To prepare the composite (Al_2O_3/Y_2O_3) gel fibers in this work, aluminum chloride hexahydrate ($Al/AlCl_3·6H_2O$), aluminum and yttrium oxide powders in aqueous solution were used by sol–gel method. The obtained results are as follows:

1. Appropriate molar ratio of aluminum powder to aluminum chloride hexahydrate to prepare spinnable precursor sol was around between 0.87 and 1.81.

2. The time of hydrolysis–condensation and gelation decreased with the increasing amount of aluminum powder, whereas the time of drawing and spinnability increased.
3. Among the prepared sols with different amounts of acid, the sols consisting of 0.18–0.26 mol ratio of acid to water were spinnable.
4. The time of hydrolysis–condensation, drawing, gelation and length of the gel fibers decreased with increasing the amounts of either acid or yttrium oxide powder.
5. Based on composition, spinnability and practical production, the sols consisting of $Al/AlCl_3{\cdot}6H_2O = 1.81$ mol ratio and 6 wt.% Y_2O_3 were determined as suitable for the preparation of fibers at pH 3.2.
6. According to rheological studies, spinnable sols behaved as Newtonian fluid and maintained this behavior up to the gelling point. Some non-spinnable sols behaved as non-Newtonian fluid and others firstly behaved as Newtonian fluid and changed then into non-Newtonian behavior.
7. Fiber drawing from the viscous sols was possible in the high viscosity range of 2000–5000 P.
8. The obtained gel fibers had a smooth surface with diameter ranging from 20 to 200 μm.
9. The composite ceramic fibers contained very fine grain (100–200 nm) after heat treatment.

Acknowledgements

The authors are thankful to Dr. Rezaie, Mrs. Faeghiniya and Mr. Sedaghat for their kind assistance and interest on this work.

References

[1] K.C. Chen, K.S. Mazdiyasni, Creep resistance of developmental polycrystalline yttrium aluminum garnet fibers, Ceram. Eng. Sci. Proc. 15 (4) (1994) 181–188.
[2] D. Hamling, Using ceramic fiber material in corrosive environments, Am. Ceram. Soc. Bull. 76 (9) (1997) 79–82.
[3] R.C. Pullar, M.D. Taylor, A.K. Bhattacharya, The manufacture of yttrium aluminum garnet fibers by blow spinning from a sol–gel precursor, J. Eur. Ceram. Soc. 18 (1998) 1759–1764.
[4] E.A. Aguilar, R.A.L. Drew, Melt extraction processing of structural Y_2O_3–Al_2O_3 fibers, J. Eur. Ceram. Soc. 20 (2000) 1091–1098.
[5] L.C. Klkein, Sol–Gel Technology for Thin Films, Fibers, Preforms, Electronics and Specialty Shapes, Noyes publications, 1988, pp. 185–187.
[6] M. Allahverdi, R.A.L. Drew, Melt-extracted oxide ceramic fibers—the fundamentals, J. Mater. Sci. 31 (1996) 1035–1042.
[7] R.B. Cass, Fabrication of continuous ceramic fiber by viscous suspension spinning process, Ceram. Bull. 70 (3) (1991) 424–429.
[8] W. Krenkel, R. Naslain, H. Schneider, High temperature ceramic matrix composites, in: Proceedings of the 4th Germany International Conference on High Temperature Ceramic Matrix Composites (HT-CMC4), 1–3 October, (2001), pp. 156–162.
[9] B.G. Muralidharan, D.C. Agrawal, Sol–gel derived TiO_2–SiO_2 fibers, J. Sol–Gel. Sci. Technol. 9 (1997) 85–93.
[10] J.D. Birchall, The preparation and properties of polycrystalline aluminum oxide fibers, Reported from New Science Group, ICI Ltd., Runcorn, 2007.
[11] G. Emig, R. Wirth, R. Zinmermann, Sol/gel-based precursor for manufacturing refractory oxide fibers, J. Mater. Sci. 29 (1994) 4559–4566.
[12] M.T. Tsai, Alkoxide sol–gel processed cordierite fiber, J. Am. Ceram. Soc. 85 (16) (2002) 1637–1639.
[13] W. Glaubitt, W. Watzka, H. Scholz, Sol–gel processing of functional and structural ceramic oxide fibers, J. Sol–Gel. Sci. Technol. 8 (1997) 29–33.
[14] R.C. Pullar, M.D. Taylor, A.K. Bhattacharya, The sintering behavior, mechanical properties and creep resistance of aligned polycrystalline yttrium aluminum garnet fibers produced from an aqueous sol–gel precursor, J. Eur. Ceram. Soc. 19 (1999) 1747–1758.
[15] A. Towata, H.J. Hwang, M. Sando, Sol–gel derived Al_2O_3 fiber dispersed with fine YAG particles, Key. Eng. Mater. 164/165 (1999) 27–30.
[16] A. Towata, H.J. Hwang, M. Yasuoka, Fabrication of fine YAG-particulate-dispersed alumina fiber, J. Am. Ceram. Soc. 81 (9) (1998) 2469–2472.
[17] K. Chang Song, Preparation of mullite fibers by the sol–gel method, J. Sol–Gel. Sci. Technol. 13 (1998) 1017–1021.
[18] K. Okada, T. Motohashi, Y. Kameshima, Sol–gel synthesis of YAG/Al_2O_3 long fibers from water solvent systems, J. Eur. Ceram. Soc. 20 (2000) 561–567.
[19] J. Yang, S.M. Jeng, S. Chang, Fracture behavior of directionally solidified $Y_3Al_5O_{12}/Al_2O_3$ eutectic fiber, J. Am. Ceram. Soc. 79 (5) (1996) 1218–1222.
[20] M. Zhanag, I.M. Miranda, D.M. Vilarinho, The effect of acid mixture on the structure of sol–gel PZT fibers, Mater. Lett. 57 (2003) 4271–4275.
[21] M.E.P. Fernandez, C. Kang, D.I. Mangonon, Process ceramic fibers by sol–gel, Chem. Eng. Prog. (1993) 49–53.
[22] R. Meyer, T. Shrout, S. Yoshikawa, Lead zirconate titanate fine fibers derived from alkoxide-based sol–gel technology, J. Am. Ceram. Soc. 81 (4) (1998) 361–368.
[23] C. Jeffry Brinker, Sol–Gel Science, The Physics and Chemistry of Sol–Gel Processing, Academic Press Limited, London, 1990, pp. 159–163.
[24] Y.H. Chiou, M.T. Tsai, The preparation of alumina fiber by sol–gel processing, J. Mater. Sci. 29 (1994) 2378–2388.
[25] M.T. Tsai, Hydrolysis and condensation of forsterite precursor alkoxides: modification of the molecular gel structure by acetic acid, J. Non-Cryst. Solids 298 (2002) 116–130.
[26] M. Zhang, I.M. Miranda, P.M. Vilarinbo, The effect of acid mixture on the structure of sol–gel PZT fibers, Mater. Lett. 57 (2003) 4271–4275.
[27] M.T. Tsai, Effects of hydrolysis processing on the character of forsterite gel fibers. Part 1. Preparation, spinnability and molecular structure, J. Eur. Ceram. Soc. 22 (2002) 1073–1083.
[28] K. Okada, S. Yasohama, S. Hayashi, Sol–gel synthesis of mullite long fibers from water solvent systems, J. Eur. Ceram. Soc. 18 (1998) 1879–1884.
[29] A. Sedaghat, E. Taheri-Nassaj, R. Naghizadeh, An alumina mat with nanomicrostructure prepared by centrifugal spinning method, J. Non-Cryst. Solids 352 (2006) 2818–2828.
[30] M.T. Tsai, Characterization of nanocrystalline forsterite fiber synthesized via the sol–gel process, J. Am. Ceram. Soc. 85 (2) (2002) 453–458.
[31] O. Yamaguchi, K. Takeoka, K. Hirato, Formation of alkoxy-derived yttrium aluminum oxides, J. Mater. Sci. 27 (1992) 1261–1264.